CHANSON, H., BUNG, D., and MATOS, J. (2015). "Stepped spillways and cascades." in "Energy Dissipation in Hydraulic Structures." IAHR Monograph, CRC Press, Taylor & Francis Group, Leiden, The Netherlands, H. CHANSON Editor, pp. 45-64 (ISBN 978-1-138-02755-8).

Chapter 3

Stepped spillways and cascades

H. Chanson[1], *D.B. Bung*[2] & *J. Matos*[3]
[1]*School of Civil Engineering, The University of Queensland, Brisbane, QLD, Australia*
[2]*Hydraulic Engineering Section, FH Aachen University of Applied Sciences, Bayernallee 9, Aachen, Germany*
[3]*Department of Civil Engineering, Architecture and Georesources, IST, Av. Rovisco Pais, Lisbon, Portugal*

ABSTRACT

A spillway system is an aperture designed to spill safely the flood waters and dissipate the turbulent kinetic energy of the flow before it rejoins the natural river channel. The construction of steps on the spillway may assist with the energy dissipation, thus reducing the size of the downstream stilling structure. The construction of stepped spillways is compatible with the placement methods of roller compacted concrete and gabions. The main characteristics of stepped spillway flows are the different flow regimes depending upon the relative discharge, the high turbulence levels and the intense flow aeration. Modern stepped spillways are characterised by a relatively steep slope and large flow rates per unit width. The chute toe velocity may be estimated using a graphical method, and the downstream energy dissipator must be designed accurately with the knowledge of the air-water flow properties. As the flow patterns of stepped spillways differ from those on smooth chutes, designers must analyse carefully stepped chute flows and their design is far from trivial.

3.1 INTRODUCTION

Dams and weirs are man-made hydraulic structures built across a river to provide water storage. During major rainfall events, large water inflows into the reservoir induce a rise in the reservoir level with the risk of dam overtopping. The spillway system is an aperture designed to spill safely the flood waters above, below or besides the dam wall. Most small dams are equipped with an overflow structure, the spillway, which includes typically a crest, a chute and an energy dissipator at the downstream end. The energy dissipator is designed to dissipate the excess in kinetic energy at the end of the spillway before it re-joins the natural stream. Energy dissipation on dam spillways is achieved usually by a standard stilling basin downstream of a steep chute in which a hydraulic jump takes place, converting the flow from supercritical to subcritical conditions, a high velocity water jet taking off from a ski jump and impinging into a downstream plunge pool, or a plunge pool in which the chute flow impinges and the kinetic turbulent energy is dissipated in turbulent recirculation. The construction of steps on the spillway chute may assist also with the energy dissipation.

The stepped channel design has been used for more than 3 millenia (Knauss 1995, Chanson 2000–2001). A significant number of structures were built with a stepped spillway systems during the 19th century through to the early 20th century

(Fig. 3.1A), when the design technique became outdated with the development of hydraulic jump stilling basin designs. Recent advances in construction materials and technology, including Roller Compacted Concrete (RCC) and polymer-coated gabion wire, led to a renewal of interest for the stepped chute design (Fig. 3.1B & 3.1C). The stepped spillway profile increases significantly the rate of energy dissipation taking place along the spillway, thus reducing the size of the downstream stilling structure. Stepped cascades are used also in water treatment plants to enhance the air-water transfer of atmospheric gases (e.g. oxygen, nitrogen) and of Volatile Organic Components (VOC).

In this chapter, the basic hydraulic characteristics of stepped spillways are reviewed. The energy dissipation and aeration characteristics are detailed, before the stepped chute design is discussed.

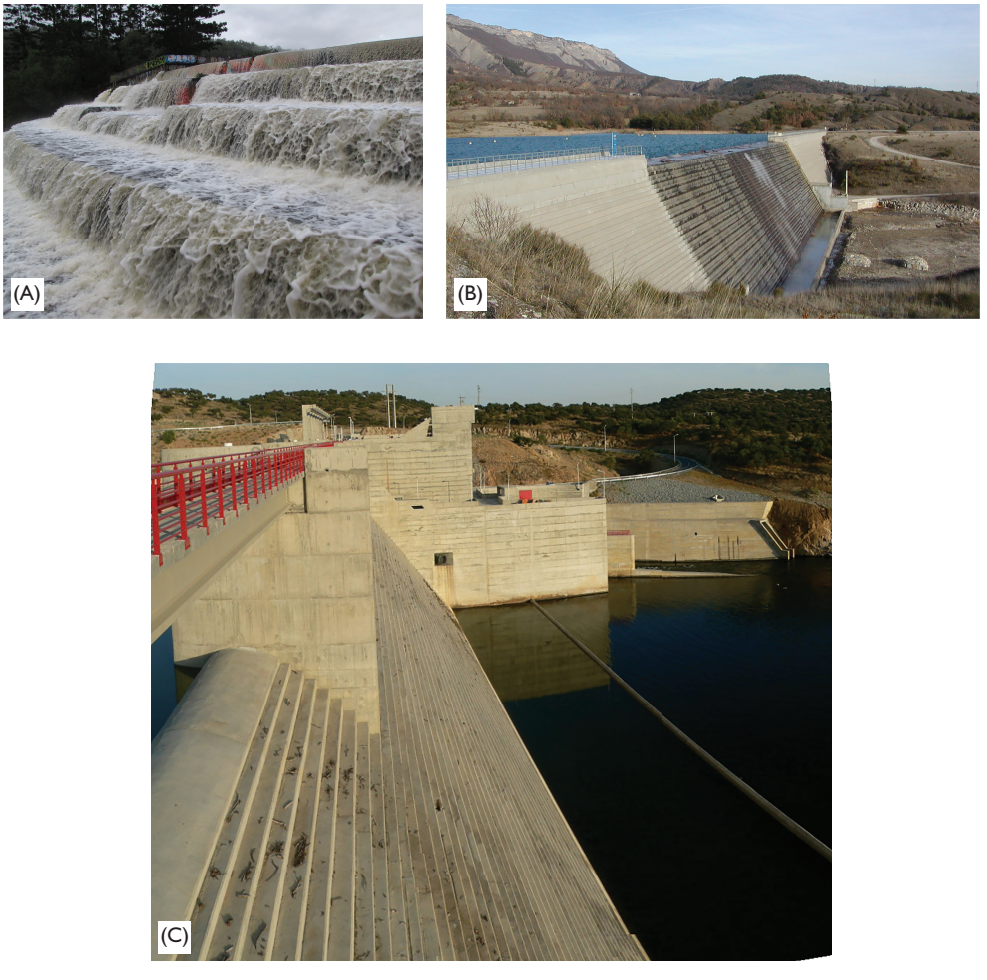

Figure 3.1 Stepped spillways. (A) Gold Creek dam stepped spillway (Australia), completed in 1890, on 14 April 2009 (Courtesy of Gordon Grigg) (B) Riou dam (France) on 11 February 2004 (C) Pedrógão dam (Portugal) on 4 September 2006.

3.2 HYDRAULICS OF STEPPED SPILLWAYS

3.2.1 Basic flow patterns

For a given stepped chute geometry, the flow may be a nappe flow at low flow rates, a transition flow for intermediate discharges or a skimming flow at larger flow rates. Figure 3.2 shows some photographs of nappe and skimming flows down a 26.6° stepped chute.

In the nappe flow regime, the flow progresses as a series of free-falling nappes impacting onto the downstream step (Fig. 3.2A). The energy dissipation occurs by jet breakup in air, jet impact onto the horizontal step face, and sometimes formation of a hydraulic jump on the step. Practical considerations show that the step height must be significantly larger than the critical flow depth (Fig. 3.3). For a range of intermediate flow rates, an intermediate flow pattern between nappe and skimming flow may be observed: the transition flow regime (Ohtsu and Yasuda 1997, Chanson and Toombes 2004). The transition flow is characterised by a chaotic flow motion associated with intense splashing. The transition flow pattern exhibits significant longitudinal variations of the flow properties at each step and between subsequent steps, and flow instabilities. It is recommended to avoid this flow regime for design operation at medium to large discharges. In a skimming flow regime, the water flows as a coherent stream, skimming over the pseudo-bottom formed by the step edges (Fig. 3.2B). Beneath the pseudo-bottom, cavity recirculation is maintained through the transfer of momentum from the main stream to the recirculating fluid.

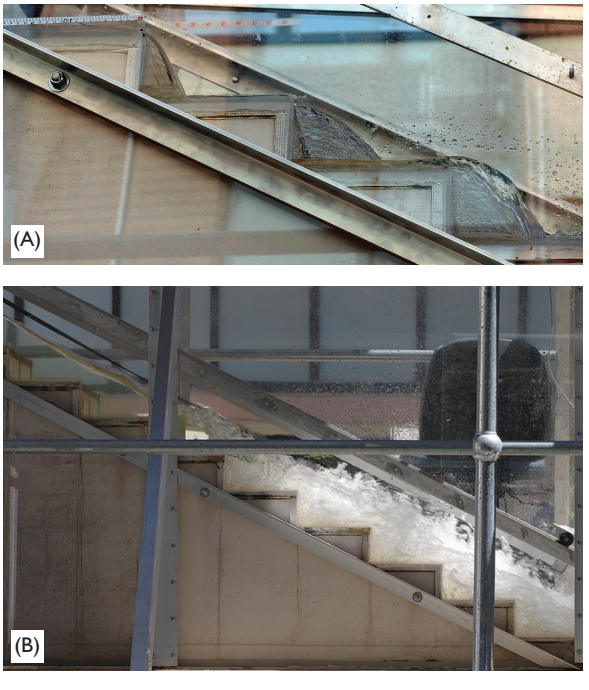

Figure 3.2 Nappe and skimming flows down a 1V:2H flat stepped chute (h = 0.10 m). (A) Nappe flow, d_c/h = 0.13. (B) Skimming flow, d_c/h = 1.45.

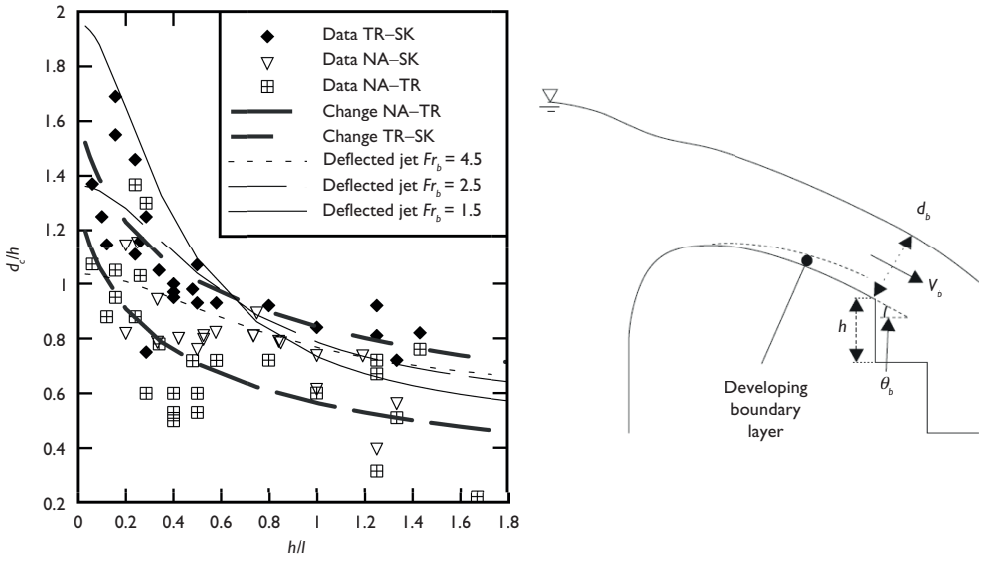

Figure 3.3 Flow conditions for the upper limit of nappe flows and lower limit of skimming flows. Comparison with older observations of transition from nappe to skimming flows. Comparison with the criterion for onset of jet deflection.

The type of flow regime is a function of the discharge and stepped configuration. The analysis of a large number of experimental observations on flat horizontal steps suggests that the upper limit of nappe flow may be approximated as

$$\left(\frac{d_c}{h}\right)_{NA-TR} = \frac{0.593}{\left(\frac{h}{l}+0.139\right)^{0.394}} \tag{3.1}$$

while a lower limit of skimming flow is given by:

$$\left(\frac{d_c}{h}\right)_{TR-SK} = \frac{0.881}{\left(\frac{h}{l}+0.149\right)^{0.317}} \tag{3.2}$$

where d_c is the critical flow depth, h is the vertical step height and l is the horizontal step length. Equations (3.1) and (3.2) are compared with experimental data in Figure 3.3 (thick dashed lines), together with older observations of the transitions between nappe and skimming flows. The results characterise a change in flow regime for quasi-uniform flows, and should not be applied to rapidly varied flows.

Some prototype and laboratory observations indicated the risk of jet deflection at the upstream steps if these are too high (Fig. 3.3 Right). A theoretical solution for the onset of jet deflection is (Chanson 1996):

$$\frac{d_c}{h} < \frac{Fr_b^{2/3} \times \sqrt{1 + \frac{1}{Fr_b^2}}}{\sqrt{1 + 2 \times Fr_b^2 \times \left(1 + \frac{1}{Fr_b^2}\right)^{3/2} \times \left(1 - \frac{\cos\theta_b}{\sqrt{1 + \frac{1}{Fr_b^2}}}\right)}} \tag{3.3}$$

where $Fr_b = V_b/(g \times d_b)^{1/2}$, d_b and V_b are the flow depth and mean velocity at the brink and θ_b the angle between the invert and horizontal. Equation (3.3) is shown in Figure 3.3 and may be used to prevent risks of jet deflection at the first steps, for example by installing smaller first steps.

3.2.2 Hydraulics of nappe flow

For a given stepped geometry, small discharges operate in the nappe flow regime (Fig. 3.2A). At each step brink, a free-falling nappe takes off with an air cavity and a pool of recirculating fluid underneath. Air entrainment may take place at the upper and lower nappes, with additional air being entrained by a plunging jet motion at the intersection of the lower nappe with the recirculating water. For low discharges and flat slopes, a hydraulic jump may take place downstream of the jet impact and upstream of the next step edge. For larger flow rates and steeper chutes, the flow is supercritical all along the spillway and no jump is observed.

The pressures and pressure fluctuations on the channel steps are important factors affecting the stepped spillway operation. Large hydrodynamic forces are exerted at the impact of the falling nappe, on the vertical face if the nappe is not adequately ventilated, and possibly beneath the hydraulic jump. At nappe impact, large invert pressures may be experienced next to the stagnation point, with mean stagnation pressure P_s about (Chanson 1995a):

$$\frac{P_s - P_{atm}}{\rho_w \times g \times h} = 1.25 \times \left(\frac{d_c}{h}\right)^{0.35} \tag{3.4}$$

and extreme maximum and minimum pressures of the order of magnitude:

$$(P_s)_{max} \approx P_s + 0.9 \times \rho_w \times \frac{V_i^2}{2} \tag{3.5}$$

$$(P_s)_{min} \approx P_s - 0.6 \times \rho_w \times \frac{V_i^2}{2} \tag{3.6}$$

with V_i the impact velocity of the falling nappe.

The nappe ventilation is essential for a proper spillway operation in the nappe flow regime. In absence of aeration, fluttering instabilities may develop associated

with oscillations of the nappe and loud noise (Fig. 3.4 Right) (Pariset 1955). The danger to the dam structure is usually small, unless the fluttering frequency is close to the resonance frequency of the system. For a stepped spillway with flat horizontal steps, the theoretical oscillation frequencies are shown in Figure 3.4 (Left) and they are compared with experimental observations including prototype spillway data. In this section, it is assumed that the nappe cavity is adequately ventilated.

In a nappe flow, the energy dissipation occurs by jet breakup and mixing, and possibly the formation of a hydraulic jump on the horizontal step face. The total head loss along the chute ΔH equals the difference between the maximum head available H_1 and the residual head H_{res} at the downstream end of the spillway. Thus the rate of energy dissipation for an ungated stepped spillway equals (Chanson 1994a):

$$\frac{\Delta H}{H_1} = 1 - \left(\frac{0.54 \times \left(\frac{d_c}{h}\right)^{0.275} + \frac{3.43}{2} \times \left(\frac{d_c}{h}\right)^{-0.55}}{\frac{3}{2} + \frac{H_{dam}}{d_c}} \right) \tag{3.7}$$

where H_{dam} is the drop in elevation between the spillway crest and chute toe. Although developed for nappe flow with hydraulic jump, Equation (3.7) was tested successfully for nappe flow without hydraulic jump and stepped chute slopes up to 23° (Chanson 2001a).

A number of design criteria were proposed for stepped cascades operating with nappe flows (Binnie 1913, Stephenson 1991). These imply relatively large steps and flat slopes, a situation not often practical although suited for some river training

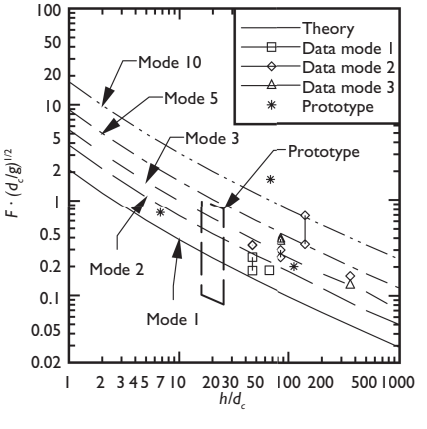

Figure 3.4 Deflected nappe oscillations. Left: comparison between theoretical calculations (Casperson 1993) and observations of nappe oscillation frequency *F*. Right: nappe oscillations at Chichester dam in April 2008: "The intake of air was quite audible, and pulsing at around five intakes per second" (Courtesy of Ken Rubeli).

and storm waterways. Practically, design engineers must size the sidewall height to prevent spray overflow. This is particularly important for embankment stepped spillways since the risk of erosion of the non-overflow section must be taken into account. A similar criterion may be used to prevent the developing spray to generate fog or ice in the surroundings in cold weather conditions.

3.2.3 Hydraulics of skimming flow

At large discharges, the water flows down a stepped spillway as a coherent stream skimming over the pseudo-bottom formed by the step edges. In the step cavities, recirculating vortices develop and the recirculation motion is maintained through the transmission of shear stress from the main flow (Fig. 3.2B). Most turbulent kinetic energy is dissipated to maintain the cavity circulation.

At the upstream end of the chute, the skimming flow free-surface is smooth and no air entrainment occurs. Once the outer edge of the developing boundary layer interacts with the free-surface, the flow is characterised by strong air entrainment. For an uncontrolled stepped spillway, the location of the inception point of free-surface aeration may be derived based upon a semi-analytical expression of the turbulent boundary layer development (Chanson 1994b,1995):

$$\frac{(L_I)_{uc}}{h \times \cos\theta} = 9.719 \times (\sin\theta)^{0.0796} \times F_*^{0.713} \tag{3.8}$$

where L_I is the streamwise distance from the crest, the subscript *uc* refers to an uncontrolled crest, θ is the angle between the chute slope ($\tan\theta = h/l$) and horizontal, and F_* is a Froude number defined in terms of the step roughness height:

$$F_* = \frac{q_w}{\sqrt{g \times \sin\theta \times (h \times \cos\theta)^3}} \tag{3.9}$$

A similar reasoning gives an expression of the flow depth at inception (Chanson 1994b):

$$\frac{(d_I)_{uc}}{h \times \cos\theta} = 0.4034 \times \frac{F_*^{0.592}}{(\sin\theta)^{0.04}} \tag{3.10}$$

For a gated spillway or a pressurised intake, the initial flow conditions of boundary layer development differ, and the analytical calculations imply (Chanson 2006):

$$\left(\frac{(L_I)_{pi}}{h \times \cos\theta}\right)^{1.4} = \left(\frac{(L_I)_{uc}}{h \times \cos\theta}\right)^{1.4} \times \frac{1}{1 + \dfrac{F_*^{2/3}}{\dfrac{(L_I)_{pi} \times (\sin\theta)^{1/3}}{h \times \cos\theta}} \times Fr_1^{-2/3} + \frac{1}{2} \times Fr_1^{4/3}} \tag{3.11}$$

$$\left(\frac{(d_1)_{pi}}{h\times\cos\theta}\right)^{1.57} = \left(\frac{(d_1)_{uc}}{h\times\cos\theta}\right)^{1.57} \times \frac{1}{1+\dfrac{F_*^{2/3}}{\dfrac{(L_1)_{pi}\times(\sin\theta)^{1/3}}{h\times\cos\theta}}\times Fr_1^{-2/3}+\dfrac{1}{2}\times Fr_1^{4/3}} \quad (3.12)$$

where the subscript *pi* refers to pressurised intake conditions and Fr_1 is the intake flow Froude number. Basic considerations show that the location of the inception point of free-surface aeration is located further upstream on a controlled chute or with a pressurised intake, for an identical flow rate, slope and step height. A number of prototype and laboratory data are shown in Figure 3.5 and compared with Equations (3.8), (3.10), (3.11) and (3.12). In skimming flows on an uncontrolled crest, the prototype data followed relatively closely Equations (3.8) and (3.10).

Flow resistance in skimming flows is associated with considerable form losses and momentum transfer between the main flow and the step cavity recirculation (Rajaratnam 1990). A comprehensive re-analysis of flow resistance data in laboratory and prototype is presented in Figure 3.6, regrouping 249 data points. Figure 3.6 presents the equivalent Darcy friction factor as function of the dimensionless cavity height $h \times \cos\theta/D_H$, where D_H is the hydraulic diameter. For steep chutes ($\theta > 10°$), the data presented no obvious correlation with the relative cavity height, Reynolds and Froude numbers (Chanson et al. 2002). Overall the data compared well with a simplified analytical model of the pseudo-boundary shear stress:

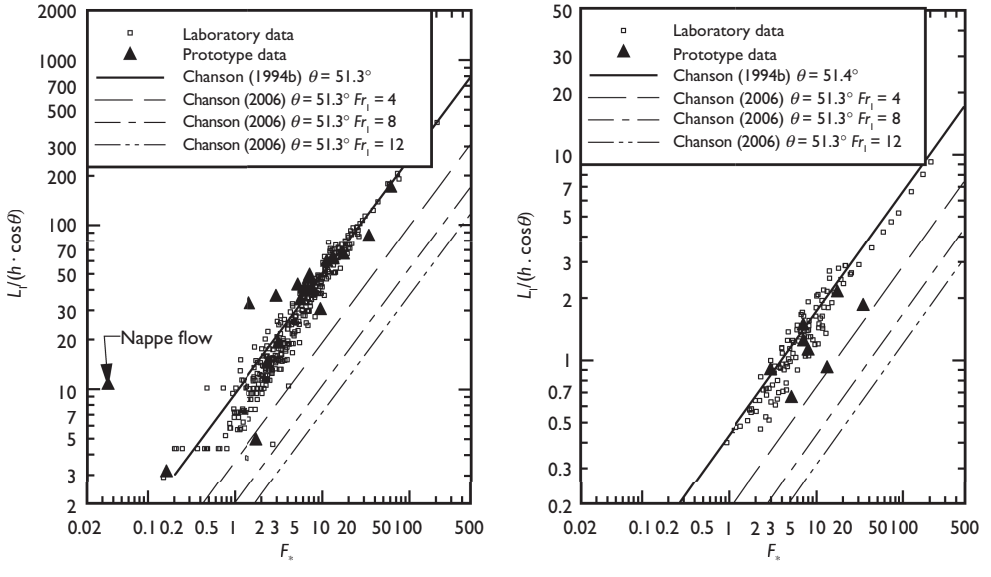

Figure 3.5 Location and flow depth at the inception point of free-surface aeration. Comparison between prototype observations (Trigomil, Dona Francisca, Pedrógão, Brushes Clough, Gold Creek, Paradise, Hinze), laboratory data, and Equations (3.8), (3.10), (3.11) and (3.12).

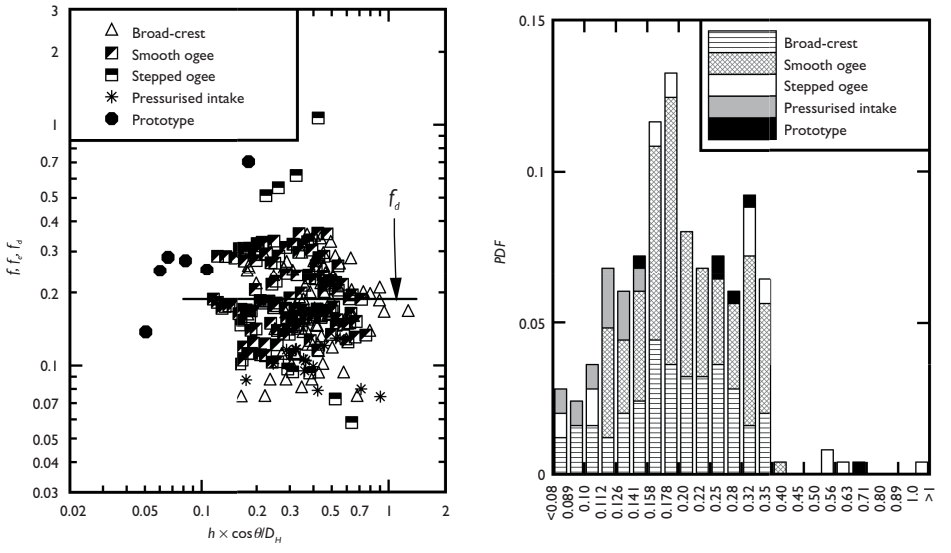

Description	*Broad-crest*	*Smooth ogee*	*Ogee with steps*	*Pressurised intake*	*Prototype*
Nb samples	86	121	19	17	6
Mean value	0.17	0.18	0.30	0.10	0.32
Range	0.07–0.35	0.10–0.36	0.06–1.1	0.07–0.13	0.14–0.70

Figure 3.6 Darcy-Weisbach friction factor in skimming flow above a stepped spillway as a function of the relative cavity height $h \times \cos\theta/D_H$ (Left) and its probability distribution function (Right) Comparison between laboratory ($\theta > 10°$, $h > 0.02$ m, $Re > 1 \times 10^5$) and prototype data.

$$f_d = \frac{2}{\sqrt{\pi}} \times \frac{1}{K} \tag{3.13}$$

with $1/K$ being the shear layer expansion rate (Rajaratnam 1976, Schlichting 1979). Equations (3.13) thus predicts $f_d \sim 0.2$ for $K = 6$, a result comparable to experimental observations (Fig. 3.6 Left).

Altogether the skimming friction factor data appeared to be distributed around three dominant values: $f \approx 0.11$, 0.17 and 0.30 as shown in Figure 3.6 Right which presents the normalised probability distribution function of friction factor. It was suggested that flow resistance in skimming flows is not an unique function of flow rate and stepped chute geometry (Chanson 2006, Felder and Chanson 2009a). The form drag process may present several modes of excitation resulting from the vortex shedding in the shear layers downstream of each step edge. A number of laboratory data showed further that the flow properties in skimming flows oscillated between adjacent step edges (Boes 2000, Matos 2000, Chanson and Toombes 2002a, Gonzalez and Chanson 2004, Felder and Chanson 2009a). The existence of such instabilities implied that the traditional concept of 'normal flow' might not exist in skimming flows on stepped spillways.

3.3 HYDRAULIC DESIGN OF STEPPED SPILLWAYS

3.3.1 Energy dissipation

A sound estimate of the residual energy head at the stepped spillway toe is essential during the design stages. Compared to a smooth invert chute, the residual energy is drastically lower but it often requires some additional downstream energy dissipator, e.g. a stilling basin. In the skimming flow regime usually considered for stepped spillway design, a strong, energy-consuming momentum transfer between the step cavity flow and the skimming water body is observed. The residual energy head H_{res} is directly linked to the friction factor f by

$$\frac{H_{res}}{H_{max}} = \frac{\left(\frac{f}{8 \times \sin\theta}\right)^{1/3} + \frac{\alpha}{2} \times \left(\frac{f}{8 \times \sin\theta}\right)^{-2/3}}{\frac{3}{2} + \frac{H_{dam}}{d_c}} \tag{3.14}$$

where $H_{max} = H_{dam} + 3/2 \times d_c$ is the maximum energy head above chute toe, θ is the chute angle and α is the kinetic energy correction factor taking into account the velocity distribution perpendicular to the pseudo-bottom (Fig. 3.8). Because of the strong turbulence, α was found to be about 1.1 (Matos 2000, Boes and Hager 2003b). The friction factor f may be taken from Figure 3.6. It must be noted that Equation (3.14) assumes quasi-uniform equilibrium flow to be achieved (Chanson 1994c). For lower dams, the residual energy must be calculated based upon the friction slope S_f (Eq. (3.16)).

Design engineers should be aware that full energy dissipation can never be achieved. A number of downstream energy dissipator designs may be considered. Commonly, standard stilling basins developed for smooth invert chutes are designed (Peterka 1958). But only few studies tested their hydraulic behavior in combination with stepped spillways (e.g. Cardoso et al. 2007, Bung et al. 2012).

3.3.2 Air entrainment

Prototype and laboratory observations highlighted the strong flow aeration on a stepped spillway. The turbulence acting next to the free-surface induces a substantial self-aeration. The flow aeration induces some flow bulking, thus requiring higher chute sidewalls, while it prevents cavitation damage. Although laboratory experiments showed the cavitation potential in skimming flows (Frizell et al. 2013), all prototype tests demonstrated an absence of cavitation damage, even for large discharges per unit width (Lin and Han 2001a), which is likely the result of air entrainment. A further application is the air-mass transfer on a stepped chute (Essery et al. 1978, Toombes and Chanson 2005).

In a skimming flow, the upstream flow is non-aerated. Downstream of the inception point of free-surface aeration, the entire water column becomes rapidly aerated as illustrated in Figure 3.7. Figure 3.7 shows some dimensionless distributions of void fraction and bubble count rate, and the data are compared with theoretical solutions of the advective diffusion equation for air bubbles and bubble count rate distributions.

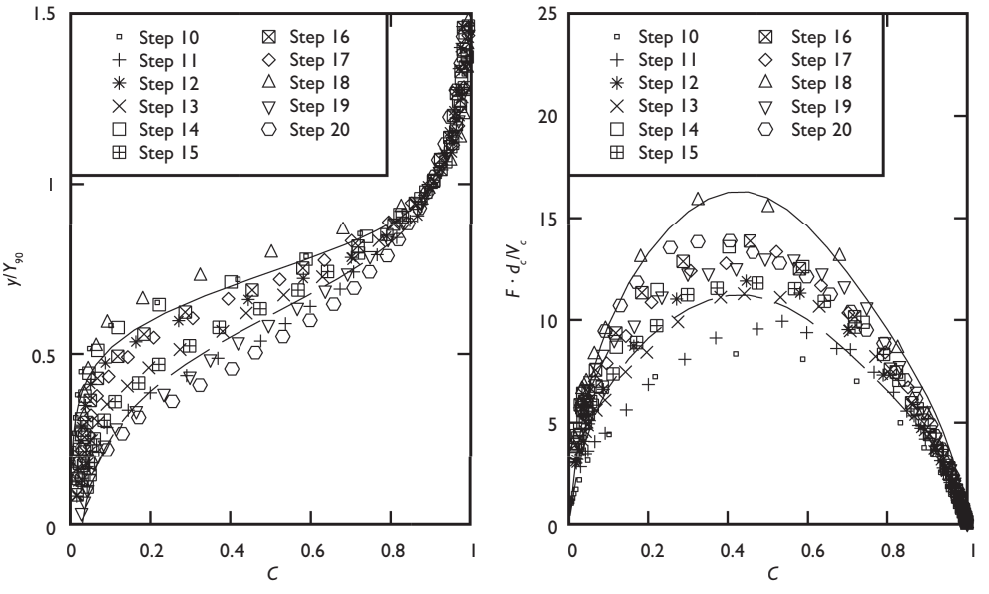

Figure 3.7 Dimensionless distributions of void fraction C (C_{mean} = 0.24 to 0.46) and bubble count rate $F \times d_c/V_c$ in skimming flows – Flow conditions: $\theta = 21.8°$, $h = 0.05$ m, $d_c/h = 1.75$ – Comparison with an advective diffusion model for air bubbles (C_{mean} = 0.25 & 0.40, Chanson & Toombes 2002b) and bubble count rate distribution model (Toombes & Chanson 2008).

3.3.3 Design guidelines

During the last four decades, a number of stepped spillways were designed for gravity dams and embankment structures (Chanson 2001a). In the 1990s, the construction of secondary stepped spillways accounted for nearly two-thirds of dam construction in USA (Ditchey and Campbell 2000). There are several construction techniques to form a stepped slope, including gabions, reinforced earth, pre-cast concrete slabs and Roller Compacted Concrete (RCC). RCC construction and gabion placement techniques yield naturally a spillway in a simple stepped fashion. Gabion stepped chutes are usually restricted to small structures (Peyras et al. 1992), while the step face roughness and seepage flow must be accounted for (Kells 1993, Gonzalez et al. 2008, Wutrich and Chanson 2014).

The stepped spillway is typically designed to operate in a skimming flow regime. During the design process, the dam height, its downstream slope and the design discharge are known parameters. The variables include the chute width and step height, possibly the flow regime. The design engineers are often limited to select a step height within the values determined by the dam construction technique (h = 0.2 to 1.2 m with RCC). Chanson (2001b) and Gonzalez and Chanson (2007) detailed the complete design steps, and a summary follows.

At design flow, the inception point of free-surface aeration must, if possible, be located upstream of the chute downstream end to ensure that the flow is

fully-developed before and minimise the residual energy at the chute toe (Fig. 3.8). The inception point characteristics may be calculated using Equations (3.8) and (3.10) for an ungated spillway and Equations (3.11) and (3.12) for a gated spillway crest.

If the spillway chute is long enough for the flow to reach uniform equilibrium, the equivalent clear-water flow depth is derived from momentum considerations:

$$d = \sqrt[3]{\frac{f \times q_w^2}{8 \times g \times \sin\theta}} \tag{3.15}$$

where the friction factor f may be estimated from Figure 3.6 for preliminary design purposes. When normal flow conditions are not achieved before the chute toe, the flow depth may be deduced from the backwater equation:

$$\frac{\partial H}{\partial x} = -S_f = -\frac{f}{8} \times \frac{q_w^2}{g \times d^3} \tag{3.16}$$

It must be noted that the depth-averaged air concentration C_{mean} may increase to more than 50% in the fully developed flow region. For the design of chute sidewall height, the characteristic depth $Y_{90} = d/(1 - C_{mean})$ may be more relevant and could reach twice the clear-water flow depth (Bung 2013). Some studies presented relevant design calculations to predict the longitudinal variations of d, C_{mean} and Y_{90} (Matos 2000, Chanson 2001a).

Alternatively the flow properties at the chute toe may be calculated with a simple design chart linking some well-documented theoretical considerations and experimental observations (Fig. 3.9). Developing flow and uniform equilibrium

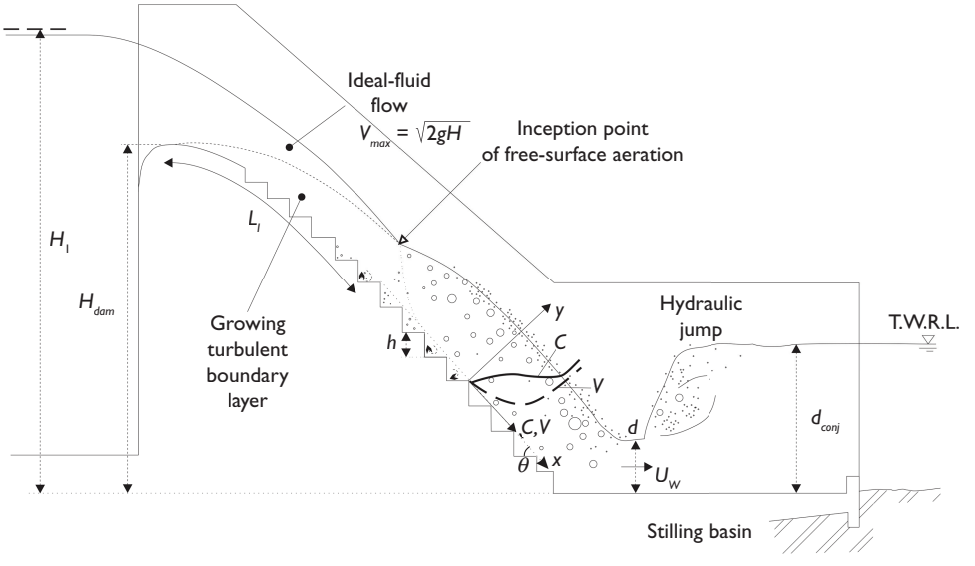

Figure 3.8 Schematic of a gravity dam stepped spillway.

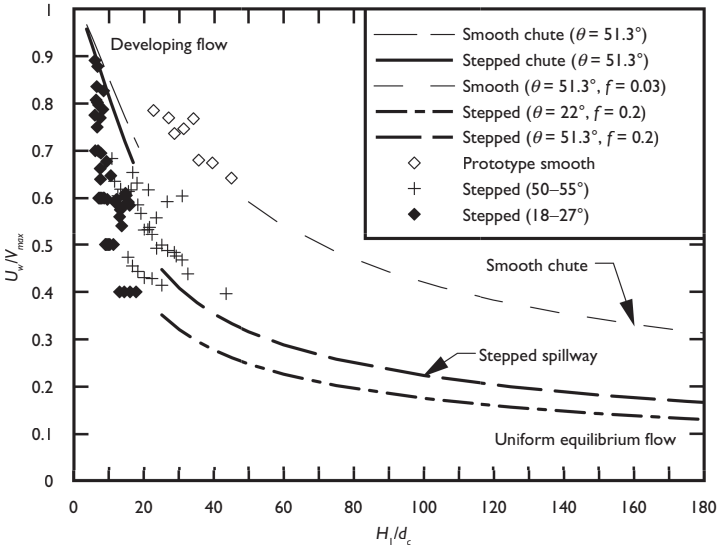

Figure 3.9 Flow velocity at the stepped spillway toe. Comparison between smooth and stepped spillway configurations.

flow calculations may be combined to provide a general trend which may be used for a preliminary design. The ideal fluid flow velocity at the downstream end of the chute is:

$$V_{max} = \sqrt{2 \times g \times (H_1 - d \times \cos\theta)} \tag{3.17}$$

where H_1 is the upstream total head above chute toe (Fig. 3.8). The flow velocity U_w at the chute toe is smaller than the ideal fluid velocity V_{max} because of the energy losses down the stepped chute. Results are summarized in Figure 3.9 in terms of U_w/V_{max} as a function of H_1/d_c where d_c is the critical depth. Developing and uniform equilibrium flow calculations are shown for both smooth chutes and uncontrolled stepped spillways for two slopes $\theta = 22°$ (1V:2.5H) and $\theta = 51.3°$ (1V:0.8H) typical of embankment and gravity dam spillways. Prototype smooth chute data and laboratory stepped spillway data are included for comparison. Despite some scatter, Figure 3.9 provides a simple means to estimate the flow velocity U_w at the chute toe as a function of flow rate and upstream total head. Overall Figure 3.9 illustrates the slower velocity and lesser residual energy at the end of a stepped spillway compared to a smooth spillway design.

In some practical cases, for small dams and for medium dams and high unit design flow, the inception point of free-surface aeration may not take place on the chute length for the design discharge. In such cases, some simple design guidelines may be based upon analytical and semi-analytical models of the non-aerated developing flow region (Chanson 2001b, Meireles and Matos 2009).

While most modern stepped spillways consists of flat horizontal steps, recent studies suggested different step configurations that might enhance the rate of energy dissipation (André et al. 2008, Gonzalez and Chanson 2008).

Designers should be aware that the stepped spillway design is a critical process, as any failure can lead to a catastrophe. A number of key parameters should be assessed properly, including flow conveyance through the crest and chute, stepped face erosion, energy dissipation above the steps and in the downstream stilling structure, interactions between the abutments and the stepped face... In turn, some physical modelling with scaling ratios no greater than 3:1 is strongly recommended, especially if the full properties of the air-water flows are of interest, including flow bulking and air-water mass transfer. A few studies systematically investigated the aerated flow properties, at the local sub-millimetre scale, in geometrically similar models under controlled flow conditions to assess the associated-scale effects. These studies were based upon Froude and Morton similarity with undistorted models of stepped spillways (Boes and Hager 2003a, Chanson and Gonzalez 2005, Felder and Chanson 2009b). Despite the limited scope, the results demonstrated the limitations of dynamic similarity and physical modelling of highly turbulent aerated flows. They emphasized further that the selection of criteria to assess scale affects is critical and should involve a range of characteristics such as void fraction distributions, turbulence intensity distributions and distributions of bubble chords (Chanson 2009). The experimental results showed that some parameters, such as bubble sizes and turbulent scales, are likely to be affected by scale effects, even in 2:1 scale models (Felder and Chanson 2009b).

3.4 PROTOTYPE EXPERIENCE

3.4.1 Prototype tests

A number of tests on prototype stepped spillway were performed in China, Russia, Germany, UK and Africa. Some extensive tests were performed on the Dachaoshan RRC dam spillway in 2002 with discharge per unit width up to 72 m^2/s (Lin and Han 2001a,b). Detailed inspections after each series of test indicated no damage nor any sign of cavitation pitting (K. Lin 2002,2012 Pers. Comm.). A series of tests conducted at the Dneiper hydroplant were performed with discharges per unit width up to 59.4 m^2/s, velocities up to 23 m/s, a step height of 0.405 m and water depths between 0.5 to 3 m (Grinchuk et al. 1977). The stability of the wedge-shaped blocks and the flow resistance was successfully tested and some flow resistance data are reported in Figure 3.6. No sign of damage and cavitation pitting was reported. Some field testing was conducted successfully on the Brushes Clough dam spillway up to 1 m^2/s, although for a short duration (Baker 2000). The data highlighted the substantial flow aeration. Some inspection of the M'Bali RCC dam stepped spillway after a wet season operation showed no sign of damage and pitting (Bindo et al. 1993).

During an uncontrolled spillway release on 2 November 1998, some pseudo-periodic, self-sustained unstabilities developed along the Sorpe dam pooled stepped spillway, the surging waters overtopping the chute sidewalls and causing a hazard to nearby tourists (Chanson 2001a, Thorwarth 2008). Some full-scale tests were

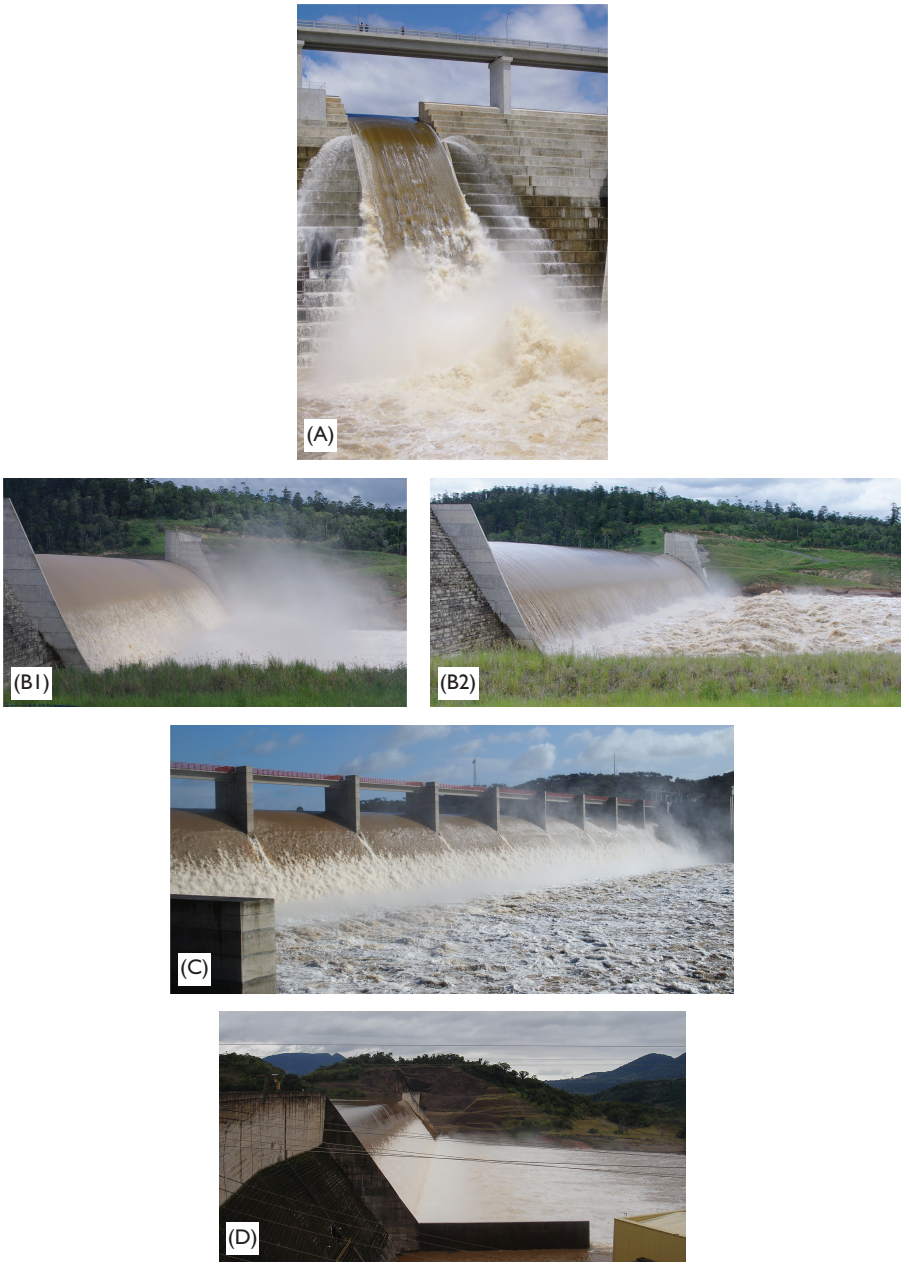

Figure 3.10 Prototype stepped spillway operations. (A) Hinze dam spillway ($\theta = 51.3°$, $h = 1.2$ m, $Q = 200$ m^3/s, $d_c/h = 2.5$ on 29 Jan. 2013). (B1) Paradise dam spillway ($\theta = 57.4°$, $h = 0.62$ m, $Q = 2{,}320$ m^3/s, $d_c/h = 2.85$ on 5 Mar. 2013). (B2) Paradise dam spillway ($\theta = 57.4°$, $h = 0.62$ m, $Q = 6{,}000$ m^3/s, $d_c/h = 5.4$ on 30 Dec. 2010). (C) Pedrógão dam ($\theta = 53.1°$, $h = 0.6$ m, on 10 Jan. 2010) (Courtesy of EDIA). (D) Dona Francisca dam ($\theta = 53.1°$, $h = 0.6$ m, in July 2011) (Courtesy of Marcelo Marques).

undertaken in 2002–2003 to investigate the jump wave occurrence and properties (P. Kamrath 2003 Pers. Comm.).

3.4.2 Discussion: Operation, experience, accidents

A number of prototype overflow events were documented worldwide (Chanson 1995a,2001a). In China, the Shuidong Hydropower Station experienced a peak flow of 90 m^2/s (He and Zeng 1995). The RCC dam spillway was protected by conventional concrete steps (h = 0.9 m) with a 8-cm chamfer. A movie documentary showed no abnormal operation and inspections after the flood event indicated no sign of damage. In Queensland (Australia), the operational record of several overflow stepped weirs demonstrated the soundness of the timber crib piled weir design. One structure, Cunningham weir, was overtopped for more than 2 months in 1956, with a maximum discharge per unit width in excess of 60 m^2/s. Only minor damage was experienced and the weir is still operational today. Between 2010 and 2013, several stepped spillways operated during a succession of major flood events. Figure 3.10 illustrates the operation of some structures. No damage to the stepped chute itself was reported despite some exceptional flood events lasting for weeks, although some scour of the Paradise dam stilling basin was documented. In two cases, the stepped spillway operated when the dam was overtopped during construction: Trigomil dam (Mexico, 1992), Cotter dam (Australia, 2012). In each case the damage was small, including for the unprotected Roller Compacted Concrete (RRC) steps. These examples are only a few and there are ample documentations on stepped spillway operations, including historical records, in Europe, Africa, America, Asia and Australia.

In hydraulic engineering, there is no better proof of design soundness than a successful operational record. This is particularly true with stepped spillway structures, in use for more than 3,500 years (Chanson 1995b,2000–2001). A number of field testings of stepped spillway structures showed a sound operation of the prototype spillways with discharges per unit width up to 72 m^2/s. These investigations are complemented by a large number of prototype experiences with stepped spillway operation during major to exceptional floods. For example, Figure 3.1A shows a 1890 staircase spillway with 1.4 m high steps which has successfully operated for over 120 years, including during large flood events. Relevant reviews of stepped spillway operation include Chanson (1995a,2001a). All the observations indicated an absence of cavitation pitting and damage to the steps. The long-lasting successful operation, for more than 3,000 years, highlights the design soundness of stepped spillways, while emphasising the importance of expert hydraulic engineering during the design stages.

3.5 CONCLUSION

The Greek hydraulic engineers were probably the first to design overflow dams with stepped spillways, more than 3,500 years ago. The overflow stepped spillways are selected to contribute to the stability of the dam, for their simplicity of shape and to reduce flow velocities. The steps increase significantly the rate of energy dissipation taking place on the steep chute and reduce the size of the required downstream energy dissipation system and the risks of scouring. The construction of stepped spillway

is compatible with the slipforming and placement methods of RCC and with the construction techniques of gabion weirs. The main characteristics of stepped spillway flows are the different flow regimes (nappe, transition, skimming) depending upon the relative discharge, the high turbulence levels and the intense flow aeration.

Modern stepped spillways are characterised by a relatively steep slope and large flow rates per unit width for which the flow spills as a skimming flow. The chute toe velocity may be estimated using a graphical method (Fig. 3.9), and the downstream energy dissipator may be designed more accurately with the knowledge of the air-water flow properties. As the flow patterns of stepped spillways differ from those on smooth chutes, designers must analyse carefully stepped chute flows. The design is far from trivial. Current expertise is focused on the hydraulics of skimming flow on prismatic rectangular channels with flat horizontal steps. Little information is available for other geometries.

ACKNOWLEDGEMENTS

The authors thank their students, former students and co-workers. They also thank all the people who provided them with relevant informations. The first author acknowledges the financial support of the Australian Research Council (Grants DP0878922 & DPDP120100481).

REFERENCES

André, S., Bollaert, J.L., and Schleiss, A. (2008). Ecoulements Aérés sur Evacuateurs en Marches d'Escalier Equipées de Macro-Rugosités – Partie 1: Caractéristiques Hydrauliques. *La Houille Blanche*, (1), 91–100 (in French).

Baker, R. (2000). Field Testing of Brushes Clough Stepped Block Spillway. In Minor, H.E. & Hager, W.H. (eds.) *Proceedings International Workshop on Hydraulics of Stepped Spillways*, Zürich, Switzerland, Balkema Publisher, 13–20.

Bindo, M., Gautier, J., and Lacroix, F. (1993). The Stepped Spillway of M'Bali Dam. *International Water Power and Dam Construction*, 45 (1), 35–36.

Binnie, A.R. (1913). *Rainfall Reservoirs and Water Supply*. Constable & Co, London, UK, 157 pages.

Boes, R.M. (2000). Zweiphasenströmung und Energieumsetzung an Grosskaskaden. (Two-Phase Flow and Energy Dissipation on Cascades.) *Ph.D. thesis*, VAW-ETH, Zürich, Switzerland (in German).

Boes, R.M., and Hager, W.H. (2003a). Two-phase flow characteristics of stepped spillways. *Journal of Hydraulic Engineering*, ASCE, 129 (9), 661–670.

Boes, R.M., and Hager, W.H. (2003b). Hydraulic design of stepped spillways. *Journal of Hydraulic Engineering*, ASCE, 129 (9), 671–679.

Bung, D.B. (2013). Non-intrusive detection of air-water surface roughness in self-aerated chute flows, *Journal of Hydraulic Research*, 51 (3), 322–329

Bung, D.B., Sun, Q., Meireles, I., Matos, J., and Viseu, T. (2012). USBR type III stilling basin performance for steep stepped spillways, *Proceedings of the 4th IAHR International Symposium on Hydraulic Structures*, APRH – Associação Portuguesa dos Recursos Hídricos, J. Matos, S. Pagliara & I. Meireles Eds., 9–11 February 2012, Porto, Portugal, Paper 4, 8 pages (CD-ROM).

Cardoso, G., Meireles, I., and Matos, J. (2007). Pressure head along baffle stilling basins downstream of steeply sloping stepped chutes. *Proceedings of 32nd IAHR Biennial Congress*, Venice, Italy, G. Di Silvio and S. Lanzoni Editors, 10 pages (CD-ROM).

Casperson, L.W. (1993). Fluttering Fountains. *Journal of Sound and Vibrations*, 162 (2), 251–262.

Chanson, H. (1994a). Hydraulics of Nappe Flow Regime above Stepped Chutes and Spillways. *Australian Civil Engineering Transactions*, I.E.Aust., CE36 (1), 69–76.

Chanson, H. (1994b). Hydraulics of Skimming Flows over Stepped Channels and Spillways. *Journal of Hydraulic Research*, IAHR, 32 (3), 445–460.

Chanson, H. (1994c). Comparison of Energy Dissipation between Nappe and Skimming Flow Regimes on Stepped Chutes. *Journal of Hydraulic Research*, IAHR, 32 (2), 213–218. Errata: 33 (1), 113.

Chanson, H. (1995a). *Hydraulic Design of Stepped Cascades, Channels, Weirs and Spillways*. Pergamon, Oxford, UK.

Chanson, H. (1995b). History of Stepped Channels and Spillways: a Rediscovery of the 'Wheel'. *Canadian Journal of Civil Engineering*, 22 (2), 247–259.

Chanson, H. (1996). Prediction of the Transition Nappe/Skimming Flow on a Stepped Channel. *Journal of Hydraulic Research*, IAHR, 34 (3), 421–429.

Chanson, H. (2000–2001). Historical Development of Stepped Cascades for the Dissipation of Hydraulic Energy. *Transactions of the Newcomen Society*, 71 (2), 295–318.

Chanson, H. (2001a). *The Hydraulics of Stepped Chutes and Spillways*. Balkema, Lisse, The Netherlands.

Chanson, H. (2001b). Hydraulic Design of Stepped Spillways and Downstream Energy Dissipators. *Dam Engineering*, 11 (4), 205–242.

Chanson, H. (2006). Hydraulics of Skimming Flows on Stepped Chutes: the Effects of Inflow Conditions? *Journal of Hydraulic Research*, IAHR, 44 (1), 51–60.

Chanson, H. (2009). Turbulent Air-water Flows in Hydraulic Structures: Dynamic Similarity and Scale Effects. *Environmental Fluid Mechanics*, 9 (2), 125–142 (DOI: 10.1007/s10652-008-9078-3).

Chanson, H., and Gonzalez, C.A. (2005). Physical modelling and scale effects of air-water flows on stepped spillways. *Journal of Zhejiang University SCIENCE*, 6A (3), 243–250.

Chanson, H., and Toombes, L. (2002a). Experimental Study of Gas-Liquid Interfacial Properties in a Stepped Cascade Flow. *Environmental Fluid Mechanics*, 2 (3), (DOI: 10.1023/A:1019884101405).

Chanson, H., and Toombes, L. (2002b). Air-Water Flows down Stepped Chutes: Turbulence and Flow Structure Observations. *International Journal of Multiphase Flow*, 27 (11), 1737–1761.

Chanson, H., and Toombes, L. (2004). Hydraulics of Stepped Chutes: the Transition Flow. *Journal of Hydraulic Research*, IAHR, 42 (1), 43–54.

Chanson, H., Yasuda, Y., and Ohtsu, I. (2002). Flow Resistance in Skimming Flows and its Modelling. *Canadian Journal of Civil Engineering*, 29 (6), 809–819.

Ditchey, E.J., and Campbell, D.B. (2000). Roller Compacted Concrete and Stepped Spillways. In Minor, H.E. & Hager, W.H. (eds.) *Proceedings International Workshop on Hydraulics of Stepped Spillways*, Zürich, Switzerland, Balkema Publisher, 171–178.

Essery, I.T.S., Tebbutt, T.H.Y., and Rasaratnam, S.K. (1978). *Design of spillways for reaeration of polluted waters*. CIRIA Report No. 72, January, London.

Felder, S., and Chanson, H. (2009a). Energy Dissipation, Flow Resistance and Gas-Liquid Interfacial Area in Skimming Flows on Moderate-Slope Stepped Spillways. *Environmental Fluid Mechanics*, 9 (4), 427–441 (DOI: 10.1007/s10652-009-9130-y).

Felder, S., and Chanson, H. (2009b). Turbulence, Dynamic Similarity and Scale Effects in High-Velocity Free-Surface Flows above a Stepped Chute. *Experiments in Fluids*, 47 (10), 1–18 (DOI: 10.1007/s00348-009-0628-3).

Frizell, K.W., Renna, F.M., and Matos, J. (2013). Cavitation Potential of Flow on Stepped Spillways. *Journal of Hydraulic Engineering*, ASCE, 139 (6), 630–636 (DOI: 10.1061/(ASCE)HY.1943-7900.0000715).

Gonzalez, C.A., and Chanson, H. (2004). Interactions between Cavity Flow and Main Stream Skimming Flows: an Experimental Study. *Canadian Journal of Civil Engineering*, 31 (1), 33–44.

Gonzalez, C.A., and Chanson, H. (2007). Hydraulic Design of Stepped Spillways and Downstream Energy Dissipators for Embankment Dams. *Dam Engineering*, 17 (4), 223–244.

Gonzalez, C.A., and Chanson, H. (2008). Turbulence and Cavity Recirculation in Air-Water Skimming Flows on a Stepped Spillway. *Journal of Hydraulic Research*, IAHR, 46 (1), 65–72.

Gonzalez, C.A., Takahashi, M., and Chanson, H. (2008). An Experimental Study of Effects of Step Roughness in Skimming Flows on Stepped Chutes. *Journal of Hydraulic Research*, IAHR, 46 (Extra Issue 1), 24–35.

Grinchuk, A.S., Pravdivets, Y.P., and Shekhtman, N.V. (1977). Test of Earth Slope Revetments Permitting Flow of Water at Large Specific Discharges. *Gidrotekhnicheskoe Stroitel'stvo*, (4), 22–26 (in Russian).

He, G., and Zeng, X. (1995). The Integral RCC Dam Design Characteristics and Optimization Design of its Energy Dissipator in Shuidong Hydropower Station. *Proceedings International Symposium on RCC Dams*, Santander, Spain, IECA-CNEGP, Vol. 1, 405–412.

Kells, J.A. (1993). Spatially Varied Flow over Rockfill Embankments. *Canadian Journal of Civil Engineering*, 20, 820–827.

Knauss, J. (1995). ΤΗΣ ΓΡΙΑΣ ΤΟ ΠΗΔΗΜΑ, der Altweibersprung. Die rätselhafte alte Talsperre in der Glosses-Schlucht bei Alyzeia in Akarnanien. *Archäologischer Anzeiger, 5*, 138–162 (in German).

Lin, K., and Han, L (2001a). Stepped Spillway for Dachaoshan RCC Dam. In Burgi, P.H. & Gao, J. (eds.) *Proceedings 29th IAHR Biennial Congress Special Seminar*, Beijing, China, SS2 Key Hydraulics Issues of Huge Water Projects, 88–93.

Lin, K., and Han, L. (2001b). Stepped Spillway for Dachaoshan RCC Dam. *Shuili Xuebao*, Beijing, China, Special Issue IAHR Congress (9), 84–87 (in Chinese).

Matos, J. (2000). Hydraulic Design of Stepped Spillways over RCC Dams. In Minor, H.E. & Hager, W.H. (eds.) *Proceedings International Workshop on Hydraulics of Stepped Spillways*, Zürich, Switzerland, Balkema Publisher, 187–194.

Meireles, I., and Matos, J. (2009). Skimming flow in the nonaerated region of stepped spillways over embankment dams. Journal of Hydraulic Engineering, ASCE, 135 (8), 685–689.

Ohtsu, I., and Yasuda, Y. (1997). Characteristics of Flow Conditions on Stepped Channels. *Proceedings of 27th IAHR Biennial Congress*, San Francisco, USA, Theme D, 583–588.

Pariset, E. (1955). Etude sur la Vibration des Lames Déversantes. (Study of the Vibration of Free-Falling Nappes) *Proceedings 6th IAHR Biennial Congress*, The Hague, The Netherlands, Vol. 3, paper C21, 1–15.

Peterka, A.J. (1958). Hydraulic Design of Stilling Basins and Energy Dissipators, *Bureau of Reclamation*, U.S. Department of the Interior, Denver.

Peyras, L., Royet, P., and Degoutte, G. (1992). Flow and Energy Dissipation over Stepped Gabion Weirs. Journal of Hydraulic Engineering, ASCE, 118 (5), 707–717.

Rajaratnam, N. (1990). Skimming Flow in Stepped Spillways. *Journal of Hydraulic Engineering*, ASCE, 116 (4), 587–591.

Schlichting, H. (1979). *Boundary Layer Theory*. McGraw-Hill, New York, USA, 7th edition.

Thorwarth, J. (2008). Hydraulisches Verhalten von Treppengerinnen mit eingetieften Stufen – Selbstinduzierte Abflussinstationaritäten und Energiedissipation. (Hydraulics of Pooled Stepped Spillways – Self-induced Unsteady Flow and Energy Dissipation.) *Ph.D. thesis*, University of Aachen, Germany. (in German).

Toombes, L., and Chanson, H. (2005). Air-Water Mass Transfer on a Stepped Waterway. *Journal of Environmental Engineering*, ASCE, 131 (10), 1377–1386.

Toombes, L., and Chanson, H. (2008). Interfacial Aeration and Bubble Count Rate Distributions in a Supercritical Flow Past a Backward-Facing Step. *International Journal of Multiphase Flow*, 34 (5), 427–436 (doi.org/10.1016/j.ijmultiphaseflow.2008.01.005).

Wutrich, D., and Chanson, H. (2014). Hydraulics, air entrainment and energy dissipation on gabion stepped weir. *Journal of Hydraulic Engineering*, ASCE, 140 (9), 04014046, 10 pages (DOI: 10.1061/(ASCE)HY.1943-7900.0000919).